Intermittent Hypoxia and Stem Cell Implants Preserve Breathing Capacity in a Rodent Model of Amyotrophic Lateral Sclerosis

Nicole L. Nichols[1], Genevieve Gowing[2], Irawan Satriotomo[1], Lisa J. Nashold[1], Erica A. Dale[1], Masatoshi Suzuki[1], Pablo Avalos[2], Patrick L. Mulcrone[1], Jacalyn McHugh[2], Clive N. Svendsen[2], and Gordon S. Mitchell[1]

[1]Department of Comparative Biosciences, University of Wisconsin, Madison, Wisconsin; and [2]Regenerative Medicine Institute and Department of Biomedical Sciences, Cedars-Sinai Medical Center, Los Angeles, California

Rationale: **Amyotrophic lateral sclerosis (ALS) is a devastating motor neuron disease causing paralysis and death from respiratory failure. Strategies to preserve and/or restore respiratory function are critical for successful treatment. Although breathing capacity is maintained until late in disease progression in rodent models of familial ALS ($SOD1^{G93A}$ rats and mice), reduced numbers of phrenic motor neurons and decreased phrenic nerve activity are observed. Decreased phrenic motor output suggests imminent respiratory failure.**

Objectives: **To preserve or restore phrenic nerve activity in $SOD1^{G93A}$ rats at disease end stage.**

Methods: **$SOD1^{G93A}$ rats were injected with human neural progenitor cells (hNPCs) bracketing the phrenic motor nucleus before disease onset, or exposed to acute intermittent hypoxia (AIH) at disease end stage.**

Measurements and Main Results: **The capacity to generate phrenic motor output in anesthetized rats at disease end stage was: (*1*) transiently restored by a single presentation of AIH; and (*2*) preserved ipsilateral to hNPC transplants made before disease onset. hNPC transplants improved ipsilateral phrenic motor neuron survival.**

Conclusions: **AIH-induced respiratory plasticity and stem cell therapy have complementary translational potential to treat breathing deficits in patients with ALS.**

Keywords: ventilatory control; respiratory plasticity; spinal cord; growth factors; motor neuron

Amyotrophic lateral sclerosis (ALS) is a devastating motor neuron disease causing paralysis and death from respiratory failure (1, 2). Decreased inspiratory muscle strength (3–5) suggests inspiratory motor neuron degeneration, although extreme inspiratory maneuvers are necessary to demonstrate functional deficits until late in ALS disease progression. Ultimately, inspiratory motor neuron death exceeds the capacity for compensation, causing ventilatory failure and ventilator dependence or death (3, 6, 7). It is essential to develop new strategies that preserve respiratory function in patients with ALS.

AT A GLANCE COMMENTARY

Scientific Knowledge on the Subject

Although ventilatory failure is the most common cause of death in amyotrophic lateral sclerosis (ALS), no treatments are available to preserve or restore breathing capacity.

What This Study Adds to the Field

We present two novel approaches: (*1*) stem cell transplants to preserve breathing capacity and (*2*) intermittent hypoxia to restore breathing capacity. These treatments slow phrenic motor neuron cell death and increase activity in spared phrenic motor neurons, respectively.

Although the pathogenesis of ALS is under active debate (8–10), one major hypothesis is that it is not cell autonomous, and that astrocytes near motor neurons contribute significantly to disease progression (11, 12). Thus, providing healthy astrocytes near motor neurons may slow motor neuron death. Others hypothesize that diminished trophic factor support contributes to motor neuron degeneration in ALS (13, 14). Because many trophic factors are neuroprotective to motor neurons, delivery of relevant growth/trophic factors may prolong motor neuron survival (13). However, clinical trials using growth factors have experienced limited success (15–19), possibly due to inadequate delivery and/or choice of growth factors.

The primary goal of the present study was to harness strategies that preserve and/or restore the capacity to increase inspiratory activity in the major nerve innervating the diaphragm (phrenic nerve) in a rat model of ALS ($SOD1^{G93A}$ mutant rats) (1, 20). First, we induced a form of brain-derived neurotrophic factor (BDNF)–dependent phrenic motor plasticity known as phrenic long-term facilitation (pLTF) with acute intermittent hypoxia (AIH) (21, 22). AIH represents a novel means of inducing new BDNF synthesis and increasing phrenic motor output (21). Second, human neural progenitor cells (hNPCs) were implanted near phrenic motor neurons to replenish functional astrocytes (23). Finally, hNPCs modified to secrete glial cell line–derived neurotrophic factor (GDNF; previously shown to slow lumbar motor neuron degeneration in $SOD1^{G93A}$ rats [24]) were implanted near phrenic motor neurons. Functional outcomes were assessed by measuring motor neuron survival and phrenic motor output at disease end stage. Some results of these studies have been previously reported in abstracts (25–27).

METHODS

Male $SOD1^{G93A}$ Sprague Dawley rats were bred to wild-type females (Taconic Laboratories, Germantown, NY) (23, 24). All experiments

(*Received in original form June 17, 2012; accepted in final form November 5, 2012*)

Supported by NIH NS057778 and the ALS Association. N.L.N. supported by NHLBI Training Grant HL007654 and the Francis Families Foundation. G.G. funded by Fonds de Recherche en Santé du Quebec (FRSQ). L.J.N. supported by NIH Training Grant RR023916.

Author Contributions: All authors contributed to the conception, design, or analysis of the study, and have approved submission of this manuscript.

Correspondence and requests for reprints should be addressed to Gordon S. Mitchell, Ph.D., Department of Comparative Biosciences, University of Wisconsin, 2015 Linden Drive, Madison, WI 53706. E-mail: mitchell@svm.vetmed.wisc.edu

This article has an online supplement, which is available from this issue's table of contents at www.atsjournals.org

Am J Respir Crit Care Med Vol 187, Iss. 5, pp 535–542, Mar 1, 2013

Originally Published in Press as DOI: 10.1164/rccm.201206-1072OC on December 6, 2012
Internet address: www.atsjournals.org

were performed on adult males at end stage (~150–180 d); end stage was defined as a 20% decrease from peak body mass.

Rats from three generations were studied, with focus on (*1*) breathing capacity measurements (Figure 1), (*2*) studies of AIH-induced pLTF (Figure 2), and (*3*) stem cell transplantation (Figures 3–6). Electrophysiology and then histochemistry were performed in all groups. Age-matched, wild-type littermates served as controls. All animal procedures were approved by the Institutional Animal Care and Use Committee at the University of Wisconsin (Madison, WI), and were in agreement with standards of the *Guide for the Care and Use of Laboratory Animals* (National Research Council, Washington, DC). The University of Wisconsin is accredited by the Association for Assessment and Accreditation of Laboratory Animal Care International (AAALAC), and is covered by National Institutes of Health (NIH) Assurance (A3368-01).

Measurements of Breathing Capacity

To assess breathing capacity, unanesthetized rats (n = 4 for $SOD1^{G93A}$ and wild-type) were placed in a whole-body plethysmograph (Buxco Electronics, Wilmington, NC) as described previously (28). Tidal volume (milliliters) and minute pulmonary ventilation (milliliters per minute) were measured during baseline and maximal chemoreceptor stimulation (inspired gas: 7% CO_2, 10.5% O_2).

Phrenic Nerve Activity

At end stage, mutant and wild-type rats were anesthetized for neurophysiological assessment of phrenic nerve activity (29). To assess integrated phrenic activity during baseline and maximal chemoreceptor activation, stable baseline conditions were established (>30 min) and the rat was then exposed to 10– to 20–mm Hg increases in end-tidal CO_2 until maximal nerve activity was achieved (arterial P_{CO_2}, ~90 mm Hg). Inspired gases were changed at 8-minute intervals; arterial blood gases were measured during baseline and 6 minutes after inspired gas changes. Wild-type (n = 18) and $SOD1^{G93A}$ rats (n = 13) were exposed to AIH. During AIH protocols, blood gases were determined as previously described (29). For rats with hNPC transplants, blood gases were tested during baseline, 20 and 40 mm Hg above baseline CO_2, and 40 mm Hg above baseline CO_2 with hypoxia.

Immunofluorescence

After neurophysiology experiments, rats were perfused and their tissues prepared for immunohistochemistry (28). After ventilatory studies, cervical (C3–C5) and thoracic (T5) spinal cord and brainstem regions containing hypoglossal motor neurons were sectioned (28). After AIH and hNPC studies, cervical sections (C3–C6) were made (24, 28). In AIH studies, primary antibodies were for neuronal nuclei (NeuN, mouse monoclonal, diluted 1:500; Chemicon, Billerica, MA), and the secondary antibody was goat anti-mouse green fluorescent Alexa 488 (diluted 1:500; Molecular Probes, Eugene, OR). In hNPC studies, primary antibodies included human-specific nuclear antigen (hNuc), choline acetyltransferase (ChAT), and anti-human cytoplasmic protein marker STEM121 (SC121, mouse monoclonal, diluted 1:2,000; StemCells Inc., Newark, CA) followed by secondary antibodies conjugated to Alexa Fluor 594 or Alexa Fluor 488 (diluted 1:500; Molecular Probes). Human GDNF immunohistochemistry was described previously (24).

Motor Neuron Counts

Using manual morphometric analyses, phrenic motor neurons were counted in the C4 ventral horn. Phrenic motor neurons were defined by a cluster of large mediolateral neurons in the C4 ventral horn (30, 31). After plethysmography and AIH studies, six C4 sections (40 μm thick) were counted. Counting criteria included a clearly defined nucleus with intact chromatin (nonpyknotic) and a cytoplasmic membrane in large cell bodies characteristic of motor neurons. The number of phrenic motor neurons in the C4 segment was extrapolated from the six sections (length of C4 phrenic motor nucleus, ~2,000 μm; 40-μm sections). After hNPC studies, 3–11 sections (35 μm thick), relatively evenly spaced along the C4 segment (2,000 μm), were visualized (24) with the ×40 objective of a fluorescence M2 imager microscope (distance between counting frames, 100 μm; frame size, 100 × 100 μm; optical dissector height, 23 μm; guard zone thickness, 2.5 μm). Only complete motor neurons with an identifiable cell body and visible 4′,6-diamidino-2-phenylindole (DAPI)–counterstained nucleus were counted. The total phrenic motor neuron number at C4 was extrapolated from the average phrenic motor neuron count per section (2,000-μm C4 segment; 35-μm sections).

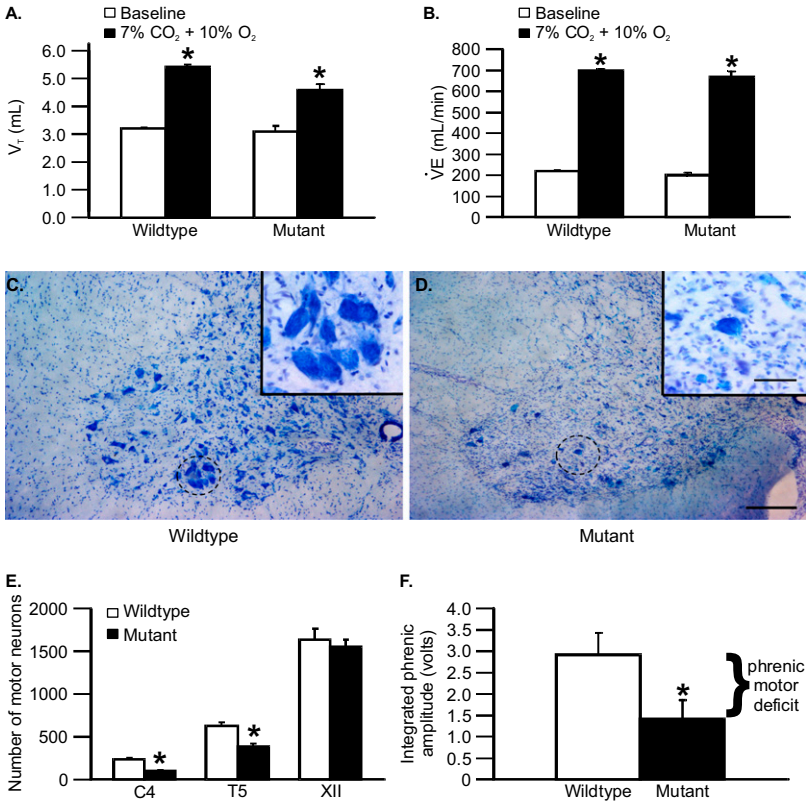

Figure 1. Breathing capacity, motor neuron survival, and phrenic activity in $SOD1^{G93A}$ rats at end stage. (*A*) Tidal volume (V_T) and (*B*) minute ventilation ($\dot{V}_E$) at baseline and during chemoreceptor stimulation (7% CO_2 + 10.5% O_2) in wild-type and mutant rats. Although chemoreceptor stimulation increased both variables (*$P < 0.05$), no differences were observed between wild-type and mutant rats. (*C* and *D*) Photomicrographs (original magnification, ×10) of (*C*) wild-type rats and (*D*) mutant rats, depicting putative phrenic motor neurons in the C4 ventral horn (framed regions where morphometric analysis was performed: original magnification, ×40). Scale bars: large panels, 200 μm; small panels, 50 μm. (*E*) Motor neuron numbers at C4 (phrenic) and T5 were significantly decreased in mutant (*solid columns*) versus wild-type rats (*open columns*) (*$P < 0.05$); hypoglossal (XII) motor neurons were unchanged ($P > 0.05$). (*F*) Integrated phrenic burst amplitude during chemoreceptor stimulation was significantly decreased in mutant (*solid column*) versus wild-type rats (*open column*; *$P < 0.05$).

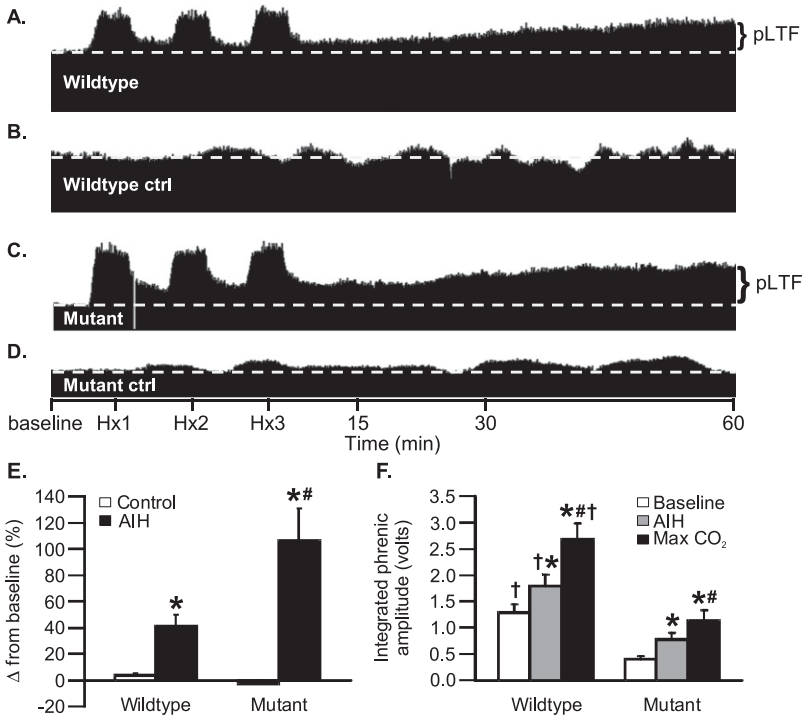

Figure 2. Acute intermittent hypoxia (AIH)–induced phrenic long-term facilitation (pLTF) in wild-type and SOD1^{G93A} rats. (*A–D*) Representative tracings of phrenic neurograms during pLTF protocol: (*A*) AIH-induced pLTF in wild-type rat; (*B*) time control (without AIH) in wild-type rat; (*C*) enhanced pLTF in mutant rat; and (*D*) time control in mutant rat. (*E*) AIH-induced pLTF in wild-type and mutant rats (change from baseline amplitude): *open columns*, time controls; *black columns*, AIH treated (*$P < 0.05$; AIH vs. time controls). pLTF was enhanced in mutant rats ($^{\#}P < 0.05$). (*F*) Integrated phrenic nerve burst amplitude was significantly larger 60 minutes post-AIH (*gray columns*) and during chemoreceptor stimulation (*black columns*) versus baseline in wild-type and mutant rats (*$P < 0.05$). Hypercapnia increased integrated phrenic amplitude versus 60 minutes post-AIH ($^{\#}P < 0.05$). Although phrenic amplitude was larger in wild-type versus mutant rats under comparable conditions ($^{\dagger}P < 0.05$), phrenic output 60 minutes post-AIH in mutant rats was not significantly different from wild-type baseline values. Hx1, Hx2, Hx3 = hypoxic episodes 1, 2, and 3, respectively.

hNPC Cultures, Lentiviral Infection, and Cell Transplantation

Methods to grow hNPCs from fetal cortex have been described (32, 33), and conform to NIH, University of Washington, and University of Wisconsin guidelines for collection of fetal tissues. Institutional review board (IRB) approval was obtained for all studies. GDNF-secreting hNPCs (hNPC-GDNF) or unaltered hNPC neurospheres were prepared for transplantation as described (23, 24, 34). To produce dead cells, hNPCs were incubated (30 min) at –80°C and thawed; live/dead cell counts confirmed 100% cell death. For transplantation, presymptomatic (110–120 d) SOD1^{G93A} rats were anesthetized, positioned in a stereotaxic frame, and laminectomy and durotomy from C3 to C6 (24) were performed. Cell injections were made as described previously (24) at C3 and C6, and then the rats were allowed to recover from surgery; the rats were carefully monitored for 2 to 3 days, and then returned to the animal facility until they reached end stage.

SOD1^{G93A} rats included hNPCs (n = 15), hNPC-GDNF (n = 12), dead hNPCs (hNPC-dead; n = 9), and nonsurgical controls (No Tx; n = 11). Nonsurgical, wild-type littermates (n = 11) were also included. Rats received cyclosporine (intraperitoneal, 10 mg/kg; Novartis) daily to prevent human cell rejection, beginning 1 day before surgery and continuing until sacrifice.

Statistical Analyses

Plethysmography data were analyzed via Buxco software (28). Integrated phrenic nerve burst amplitudes were averaged over 1 minute during baseline; 15, 30, and 60 minutes post-AIH or baseline; and maximal output. Phrenic nerve burst amplitude is reported as the voltage of the integrated signal (*see* Figure E1 for validation of measurement), as the ipsilateral-to-contralateral ratio or as a percentage change from baseline. Statistical comparisons between treatment groups for plethysmography, maximal phrenic activity, and AIH studies were done by two-way analysis of variance (ANOVA) with repeated measures design. One-way ANOVA was used to compare (*1*) integrated phrenic activity at baseline or 60 minutes post-AIH, (*2*) maximal phrenic activity in wild-type versus SOD1^{G93A} rats, and (*3*) histology data. After ANOVAs, individual comparisons were made using Student-Newman-Keuls or Fisher least significant difference (LSD) post hoc tests (SigmaPlot version 12.0; Systat Software Inc., San Jose, CA). For integrated phrenic nerve burst amplitudes (voltage) and ipsilateral-to-contralateral voltage ratios in hNPC studies, a split plot analysis with repeated measures was done (SAS or Statistical Analysis Software version 9.1.3; SAS Institute Inc.). All differences between groups were considered significant if $P < 0.05$; all values are expressed as means ± 1 SEM. Multiple linear regression analyses were performed between baseline or maximal phrenic activity with phrenic motor neuron counts.

RESULTS

Breathing Capacity Is Maintained in Unanesthetized SOD1^{G93A} Rats at End Stage

Combined hypercapnia and hypoxia was used to elicit a standardized level of increased ventilatory drive, enabling assessment of the capacity to increase inspiratory volume (28). Measurements were made when SOD1^{G93A} rats reached end stage (20% decrease from peak body mass) and in age-matched, wild-type littermates. No significant differences were observed between SOD1^{G93A} (n = 4) and wild-type rats (n = 4) in tidal volume (milliliters) or minute ventilation (milliliters per minute) when breathing air or during chemoreceptor stimulation (Figures 1A and B). Thus, the capacity to generate inspiratory volume is preserved in end-stage SOD1^{G93A} rats at a time when limb paralysis is already severe.

Decreased Inspiratory Motor Neuron Counts

Cervical (C4; phrenic), thoracic (T5; intercostal), and hypoglossal motor neuron counts in SOD1^{G93A} and wild-type rats at end stage revealed major losses of phrenic (large, pyramidal-shaped cells in the medioventral gray matter at C4 [30]) and T5 motor neurons in SOD1^{G93A} rats (Figures 1C–1E). Motor neuron degeneration was not observed in the hypoglossal motor nucleus, which maintains upper airway patency (Figure 1E). Because the capacity to increase inspiratory volume is preserved despite major inspiratory motor neuron loss, unknown mechanisms of compensatory plasticity preserve breathing capacity at end stage in SOD1^{G93A} rats.

Decreased Phrenic Motor Output

Integrated phrenic nerve activity (28) was assessed in anesthetized SOD1^{G93A} and wild-type rats during baseline (normocapnia, hyperoxia) and maximal chemoreceptor stimulation (arterial $P_{CO_2} \geq 90$ mm Hg) at end stage. Phrenic burst amplitude

was significantly decreased during maximal chemoreceptor stimulation (Figure 1F). Collectively, in all groups of SOD1^{G93A} rats presented here (Figures 2 and 3), phrenic burst amplitude was significantly decreased during both baseline and maximal chemoreceptor stimulation. Deficits in phrenic nerve activity suggest that motor neuron cell death will eventually exceed the capacity for compensation, resulting in ventilatory failure as shown in a murine ALS model (35).

Acute Intermittent Hypoxia Restores Phrenic Motor Output

Phrenic long-term facilitation (pLTF) is expressed as a prolonged increase in phrenic motor output after AIH (three 5-min hypoxic episodes; PaO_2, ~35 to 45 mm Hg; 5-min intervals) in wild-type rats (21, 22) (Figures 2A and 2B). In end-stage SOD1^{G93A} rats, pLTF was significantly greater in SOD1^{G93A} versus wild-type rats 60 minutes post-AIH (Figures 2C–2E). AIH increased phrenic activity in end-stage SOD1^{G93A} rats (Figure 2F) to levels equal to baseline levels in wild-type rats (in volts; Figure 2F), demonstrating that AIH restored phrenic motor output to normal levels in this model.

hNPC Transplantation Preserves Phrenic Motor Output

To establish whether hNPCs (with or without GDNF release) preserve phrenic motor output in SOD1^{G93A} rats, bilateral phrenic nerve activity was recorded under baseline conditions and graded chemoreceptor stimulation at end stage (Figure 3). In SOD1^{G93A} rats without treatment or receiving dead hNPCs, integrated phrenic activity was significantly decreased at baseline (Figure 4A) and during maximal chemoreceptor stimulation (Figure 4B); thus dead cells have no beneficial effects. In contrast, maximal integrated phrenic activity ipsilateral to hNPC transplants was significantly greater than in SOD1^{G93A} rats without treatment or receiving dead hNPCs, and was no longer significantly different from wild-type rats (Figure 4B). Both hNPCs and hNPC-GDNF transplants significantly increased the ipsilateral-to-contralateral ratio of integrated phrenic bursts (Figures 4C and 4D) at baseline. However, only hNPCs significantly increased this ratio during chemoreceptor stimulation (Figures 4C and 4D). A ratio of about 2 with hNPC transplants (baseline and maximal) indicates full preservation (or restoration) of phrenic activity on the side of hNPC implantation because the normal decrement at end stage is about 50%. Thus, hNPCs preserved phrenic activity at wild-type levels, although GDNF secretion had no additional benefit.

hNPCs Increase Phrenic Motor Neuron Survival

hNPC survival and migration. At end stage, surviving phrenic motor neurons were surrounded by hNPCs labeled with a human-specific antibody for human nuclear protein (Figures 5A–5C). When visualizing hNPCs with the human-specific antibody, they were differentiated into astroglial-like cells, with processes extending around motor neurons (Figures 5D and 5E). Double labeling with astrocyte (glial fibrillary acidic protein [GFAP]) and progenitor (nestin) markers revealed that most cells migrating from the transplant were not mature astrocytes but, rather, immature, nestin-positive cells as described previously (24). We did not see any neurons maturing from these grafts, as described previously (24). Increased GDNF immunoreactivity was detected surrounding GDNF-secreting hNPCs (Figure 5F).

hNPCs and phrenic motor neuron survival. Phrenic motor neurons were identified as large ChAT$^+$ neurons in a cluster located in the mediolateral ventral horn at C4, as previously identified by retrograde tracer studies (30, 31). The number of phrenic motor neurons was significantly decreased in end-stage SOD1^{G93A} rats (Figure 6A; also Figure 1). hNPC transplants significantly increased phrenic motor neuron counts (Figure 6A), indicating decreased cell death. hNPC-GDNF transplants had no significant effect, although there was an insignificant trend toward greater phrenic motor neuron survival (Figure 6A). Dead hNPCs exaggerated phrenic motor neuron loss (Figure 6A), suggesting unique effects of dead human cells, possibly due to inflammatory responses.

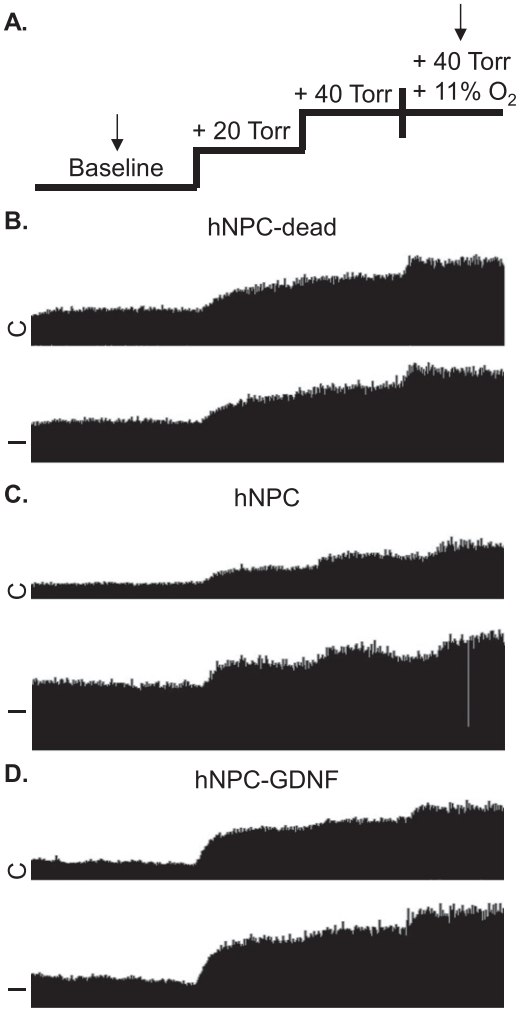

Figure 3. Phrenic neurograms after human neural progenitor cell (hNPC) transplantation in end-stage SOD1^{G93A} rats. (*A*) Experimental protocol: baseline for 15–20 minutes followed by 5-minute hypercapnia exposures (+20 and +40 mm Hg end-tidal P_{CO_2}), and hypercapnia plus hypoxia (+40 mm Hg plus 11% inspired O_2; *arrows* designate points at which data were obtained). (*B*) Ipsilateral (I) and contralateral (C) phrenic neurograms from an end-stage SOD1^{G93A} rat that had received dead hNPC (hNPC-dead) implant; I and C phrenic neurograms are nearly identical. (*C*) Ipsilateral (I) and contralateral (C) phrenic neurograms from an end-stage SOD1^{G93A} rat that received hNPC implant; I is larger than C. (*D*) Ipsilateral (I) and contralateral (C) phrenic neurograms from a mutant rat that received hNPCs secreting glial cell line–derived neurotrophic factor (hNPC-GDNF) implant; I slightly larger than C.

hNPCs and nonphrenic motor neuron survival. There were also reduced numbers of nonphrenic motor neurons in the C4 segment at end stage (Figure 6B). However, in contrast to phrenic motor neurons, ipsilateral counts of nonphrenic motor neurons were significantly increased by GDNF-secreting hNPCs, but not hNPCs alone. Thus, GDNF exerts beneficial effects on nonphrenic cervical motor neurons, similar to a previous study on

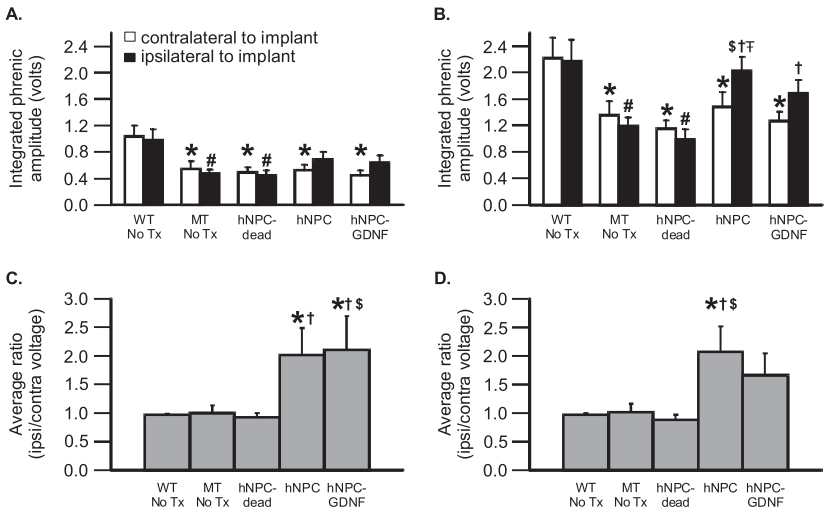

Figure 4. Unilateral human neural progenitor cell (hNPC) transplants increase ipsilateral phrenic burst amplitude (*A* and *C*) at baseline and (*B* and *D*) during chemoreceptor stimulation. Average activity (volts; *A* and *B*) and the ipsilateral-to-contralateral ratio of phrenic activity (ipsi/contra; *C* and *D*) are shown. The following groups were compared: wild-type (WT) with and without treatment (No Tx), SOD1^{G93A} (MT) rats without treatment, MT rats with dead hNPCs (hNPC-dead), MT rats with unaltered hNPCs, and MT rats with hNPCs secreting glial cell line–derived neurotrophic factor (hNPC-GDNF). Average results for ipsilateral sides (*solid columns*) and contralateral sides (*open columns*) are shown. In (*A*) baseline and (*B*) chemoreceptor stimulation, contralateral voltage was significantly lower in MT versus WT rats in all treatment groups ($*P < 0.05$). Ipsilateral voltages of MT-No Tx and hNPC-dead were significantly lower than in WT rats ($^{\#}P < 0.05$) at (*A*) baseline and (*B*) during stimulation. Ipsilateral voltages were significantly higher in hNPC and hNPC-GDNF rats versus hNPC-dead rats during stimulation ($^{\dagger}P < 0.05$) (*B*). Ipsilateral voltages with hNPCs were significantly greater versus MT-No Tx ($^{\$}P < 0.05$) during stimulation (*B*). Ipsilateral voltages with hNPCs were significantly greater than untreated contralateral sides ($^{\mp}P < 0.05$) with stimulation (*B*). hNPCs and hNPC-GDNF both increased the ipsi/contra ratio under baseline conditions ($*P < 0.05$ vs. WT rats; *C*), but only hNPCs increased the ratio during chemoreceptor stimulation ($*P < 0.05$ vs. WT rats; *D*). hNPCs and hNPC-GDNF increased the ipsi/contra ratio versus hNPC-dead rats at baseline, but only hNPCs increased the ratio during chemoreceptor stimulation ($^{\dagger}P < 0.05$). hNPC-GDNF increased the ratio at baseline versus MT-No Tx only; hNPCs also increased the ratio during stimulation versus MT-No Tx ($^{\$}P < 0.05$).

lumbar motor neurons (24), but unlike the phrenic motor neurons studied here (Figure 6B).

Correlation between Phrenic Nerve Activity and Motor Neuron Survival

Significant positive correlations were detected between integrated phrenic nerve activity and phrenic motor neuron counts ipsilateral to hNPC injections during baseline (slope = 0.32; $R^2 = 0.12$; $P < 0.05$; Figure 6C) and chemoreceptor stimulation (slope = 0.98; $R^2 = 0.15$; $P < 0.05$; Figure 6D). As expected, neither baseline nor chemoreceptor-stimulated phrenic activity correlated with contralateral motor neuron survival ($P > 0.05$). Although hNPCs may preserve the capacity to increase phrenic nerve activity via modest increases in phrenic motor neuron

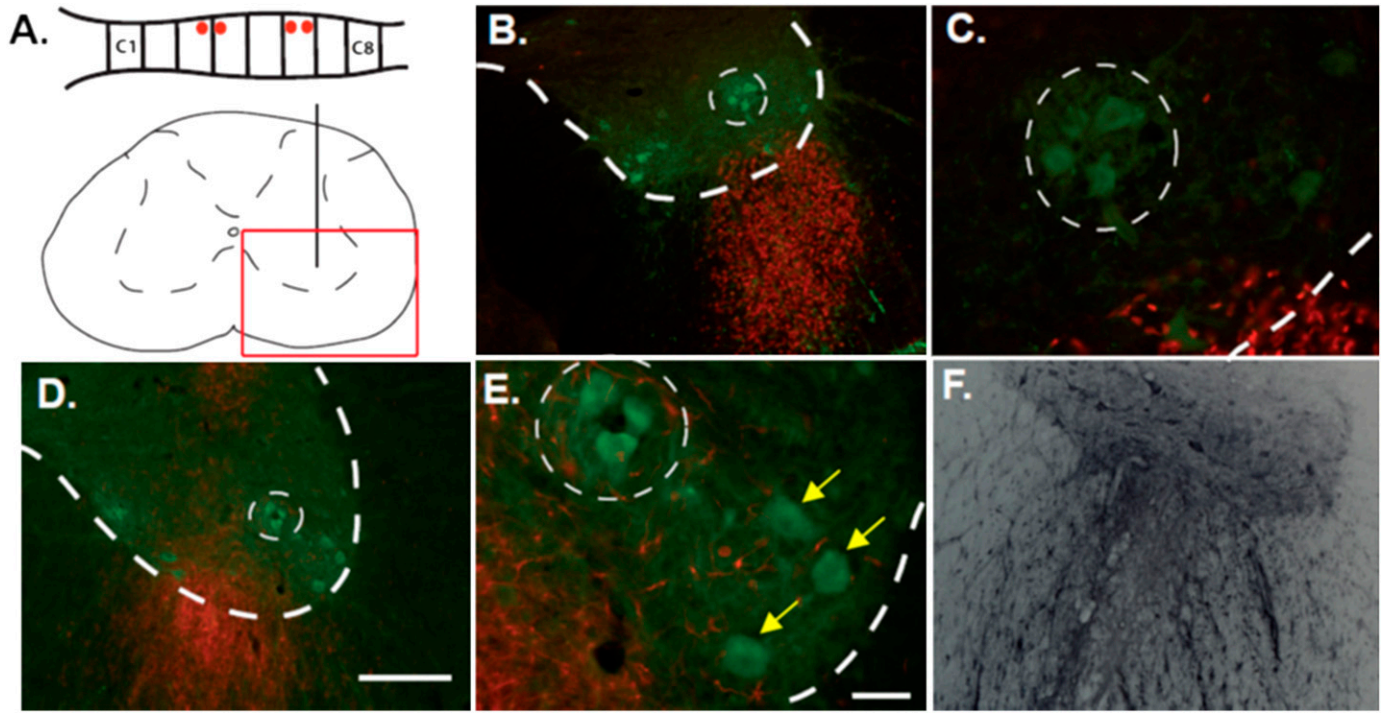

Figure 5. Motor neuron survival after human neural progenitor cell (hNPC) transplants. (*A*) Schematic of transplant sites (*red dots, vertical black lines*) and image acquisition sites (*red box*). (*B* and *C*) Immunofluorescence for choline acetyltransferase (ChAT; *green*) and human-specific nuclear antigen (hNuc; *red*). (*D* and *E*) Immunofluorescence for ChAT (*green*) and SC121 (*red*). (*B–E*) Images show distribution of grafted cells labeled with hNuc or SC121 in the ventral horn; *dotted lines* delineate the phrenic motor nucleus. *Yellow arrows* are pointing to nonphrenic motor neurons. (*F*) Light immunohistochemistry for glial cell line–derived neurotrophic factor (GDNF), demonstrating the capacity of hNPC-GDNF to secrete GDNF. Scale bars: (*D*) 200 μm (at ×10); (*E*) 50 μm (at ×40).

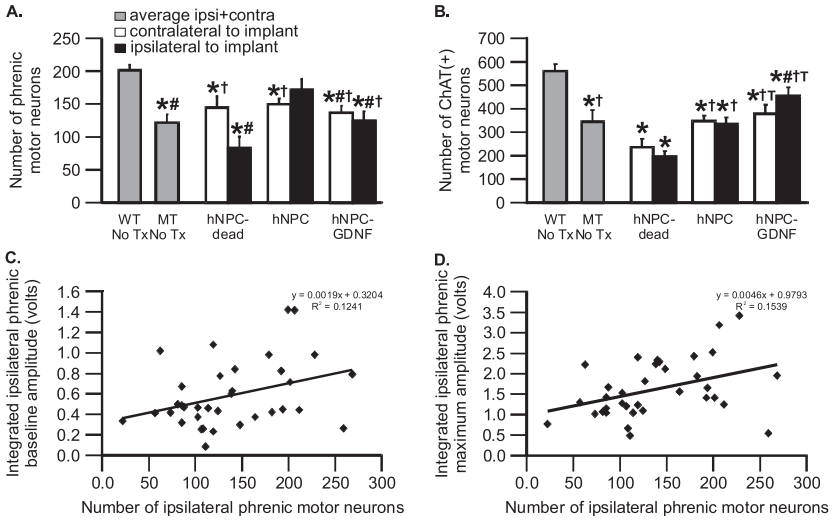

Figure 6. Surviving choline acetyltransferase–positive ($ChAT^+$) phrenic motor neurons (*A*) and nonphrenic $ChAT^+$ motor neurons in C4 ventral horn (*B*) in wild-type rats (WT), mutant rats (MT) without treatment (*gray columns*), and MT rats with human neural progenitor cell (hNPC)-dead, hNPCs, or hNPC-glial cell line–derived neurotrophic factor (GDNF) ipsilateral (*black columns*) and contralateral (*open columns*) to transplants. (*A*) MT rats without treatment, with hNPC-dead (ipsilateral and contralateral), hNPCs (contralateral), or hNPC-GDNF (ipsilateral and contralateral) had significantly fewer phrenic motor neurons versus WT rats ($^*P < 0.05$). hNPC-treated MT rats had significantly more phrenic motor neurons versus MT rats without treatment (ipsilateral), hNPC-dead (ipsilateral), or hNPC-GDNF (ipsilateral and contralateral) ($^{\#}P < 0.05$). MT rats with hNPC-dead had fewer ipsilateral phrenic motor neurons versus the contralateral side ($^{\dagger}P < 0.05$). hNPC-dead (ipsilateral) also had fewer phrenic motor neurons versus hNPCs (contralateral) and hNPC-GDNF (ipsilateral and contralateral) ($^{\dagger}P < 0.05$). (*B*) MT rats without treatment, and both ipsilateral and contralateral hNPC-dead, hNPCs, and hNPC-GDNF had fewer nonphrenic motor neurons versus WT rats ($^*P < 0.05$). Ipsilateral hNPCs had fewer nonphrenic motor neurons versus ipsilateral hNPC-GDNF ($^{\#}P < 0.05$). Ipsilateral hNPC-dead had fewer nonphrenic motor neurons versus MT rats without treatment, ipsilateral and contralateral hNPCs, and ipsilateral and contralateral hNPC-GDNF ($^{\dagger}P < 0.05$). Contralateral hNPC-dead had significantly fewer nonphrenic motor neurons versus ipsilateral and contralateral hNPC-GDNF ($^{T}P < 0.05$). Significant correlations exist between ipsilateral baseline (*C*) chemoreceptor-stimulated (*D*) phrenic nerve activity versus the number of surviving phrenic motor neurons (both regressions, $P < 0.05$).

survival, this effect is not sufficient to account for all of the increase in phrenic motor output (Figures 3–5). Other possible mechanisms of improved function include improved motor neuron health or hNPC-induced motor plasticity.

DISCUSSION

Despite major inspiratory motor neuron loss, breathing capacity is preserved in end-stage $SOD1^{G93A}$ rats. This observation demonstrates that remarkable compensatory strategies preserve this critical homeostatic function during disease progression. However, there are signs of imminent respiratory failure, expressed as diminished capacity to generate phrenic nerve activity. Eventually, compensation will be inadequate, and progressive motor neuron death will cause overt ventilatory failure (3, 5–7, 35). It is essential to find new strategies that preserve and/or restore lost phrenic motor function before we can successfully treat patients with ALS.

Here, we demonstrate the potential of two novel strategies to treat respiratory insufficiency: (*1*) induction of phrenic motor plasticity with intermittent hypoxia, and (*2*) improving phrenic motor neuron survival and function via neural progenitor cell transplants. These strategies are complementary, and have considerable translational potential to treat breathing deficits in ALS.

Respiratory Function in Rodent ALS Models

Despite its importance to the survival of patients with ALS, little is known concerning the impact of disease progression on breathing capacity in animal models of ALS. In $SOD1^{G93A}$ rats, phrenic motor neuron degeneration, diminished compound diaphragm action potentials, phrenic nerve fiber loss, and diaphragm atrophy are reported at disease end stage (36). Despite this suggestive evidence of respiratory compromise, functional deficits in the ability to generate inspiratory volume were not assessed in their study (36). Further, the ability to generate inspiratory volume is maintained until late in disease progression in $SOD1^{G93A}$ mice, but tidal volume falls abruptly over the next 1–2 days (35); respiratory motor neuron degeneration was not reported in their study.

Spontaneous Compensatory Respiratory Plasticity

Spontaneous compensatory plasticity may delay ventilatory failure in patients with ALS, despite major respiratory motor neuron loss. Possible compensatory mechanisms include (*1*) central neural plasticity, amplifying respiratory motor output from surviving motor neurons; (*2*) motor end plate sprouting in surviving phrenic motor neurons, functionally increasing the size of diaphragm motor units; and/or (*3*) shifting inspiratory functions from the diaphragm to other inspiratory muscles. This last strategy is intrinsically limited because motor neuron death is also observed in other inspiratory motor pools. An understanding of spontaneous compensatory plasticity may have major health implications because it may guide the development of novel therapeutic interventions to slow or reverse breathing deficits in ALS.

Induced Plasticity to Restore Respiratory Function

Functional benefits may be achieved by inducing further plasticity, such as AIH-induced pLTF (22). This is the first report of pLTF in any ALS model. In fact, pLTF was enhanced in end-stage $SOD1^{G93A}$ rats, restoring most of the capacity to generate phrenic motor output. Thus, intermittent hypoxia may be an interesting and simple means of restoring lost breathing capacity in ALS, similar to its application after cervical spinal injury (28, 37). Mechanisms enhancing AIH-induced pLTF in end-stage $SOD1^{G93A}$ rats are not yet known.

Because BDNF is critical for AIH-induced pLTF (21), BDNF may be sufficient to preserve phrenic motor function in end-stage $SOD1^{G93A}$ rats. Because repetitive AIH restores respiratory and nonrespiratory motor function after cervical spinal injury (28), repetitive AIH may be a simple means of up-regulating endogenous growth/trophic factors to promote phrenic motor neuron survival and function (e.g., BDNF, vascular endothelial growth factor, and erythropoietin) (21, 38, 39). At present, no data are available concerning the hypothesis that repetitive AIH elicits neuroprotective responses in respiratory or nonrespiratory motor neurons.

To date, there has been limited success in administering BDNF in clinical trials (17–19). It is possible that BDNF delivery may

cause TrkB down-regulation, or that TrkB may already be activated maximally. In contrast, both BDNF and TrkB are up-regulated by repetitive AIH (40), suggesting that AIH may represent a highly novel means of "delivering" BDNF without receptor down-regulation. On the other hand, truncated TrkB.T1 receptor deletion delays disease onset and muscle weakness in $SOD1^{G93A}$ mice, although disease end stage remained unchanged (41); this finding is consistent with at least some negative BDNF effects.

Preserving Respiratory Function with hNPCs

Another strategy to preserve or restore phrenic motor output during ALS is to provide healthy cells that effectively "repair" the environment surrounding phrenic motor neurons. We used human fetal neural progenitor cells that produce mainly astrocyte-like cells and protect motor neurons in the lumbar spinal cord of $SOD1^{G93A}$ rats, but only when expressing GDNF (23, 24). Here, we found that hNPCs improve phrenic motor neuron output and survival, without additional benefit from GDNF (Figures 3–5). Thus different motor neuron pools appear to be differentially responsive to GDNF and astrocyte replacement, possibly related to their location or function (42, 43). Indeed, considerable heterogeneity exists in spinal motor neuron properties (44–46).

Mechanisms whereby hNPCs protect phrenic motor neurons and restore phrenic activity are not known. Although hNPCs differentiate into astrocyte-like cells in the spinal cord (24), longer times are necessary to mature into fully functional GFAP-expressing astrocytes (47, 48). hNPC transplantation in the lumbar spinal cord does not reduce astrocytosis or activate microglia, suggesting that their beneficial effects arise via other mechanisms (24). Other mechanisms that could cause the effects observed here include (but are not limited to) the following: (*1*) wild-type hNPCs could increase glutamate uptake; (*2*) wild-type hNPCs could release beneficial growth/trophic factors other than GDNF; and/or (*3*) phrenic motor neurons may lack a GDNF response because the phrenic motor nucleus lacks GDNF receptors.

Possible Significance

Because patients with ALS eventually develop ventilatory failure, new strategies to delay respiratory motor neuron death and enhance the functional capacity of spared motor neurons via induced respiratory plasticity are desirable. Here we demonstrate that mechanisms increasing function in surviving motor neurons (AIH-induced plasticity) or slowing phrenic motor neuron death (hNPCs) may be viable treatment strategies. AIH is noninvasive, simple to perform, and has minimal risk of adverse effects (currently used protocols are modest in number and severity of hypoxic episodes [22]). Indeed repetitive AIH has considerable potential in the treatment of both respiratory (22, 28) and nonrespiratory motor disorders/deficits (28, 49). Further, an ongoing clinical trial using neural stem cell transplants in patients with ALS is beginning to incorporate injections near respiratory motor pools (50, 51). Combinatorial strategies involving hNPC transplants and repetitive intermittent hypoxia represent viable (and complementary) strategies to preserve/restore functional deficits in ALS.

Author disclosures are available with the text of this article at www.atsjournals.org.

Acknowledgment: The authors thank Peter Crump for statistical advice, Kalen Nichols for help with blood gas analysis, and Antonio Punzo for technical support.

References

1. Kiernan MC, Vucic S, Cheah BC, Turner MR, Eisen A, Hardiman O, Burrell JR, Zoing MC. Amyotrophic lateral sclerosis. *Lancet* 2011; 377:942–955.
2. Zinman L, Cudkowicz M. Emerging targets and treatments in amyotrophic lateral sclerosis. *Lancet Neurol* 2011;10:481–490.
3. Lyall RA, Donaldson N, Polkey MI, Leigh PN, Moxham J. Respiratory muscle strength and ventilatory failure in amyotrophic lateral sclerosis. *Brain* 2001;124:110–118.
4. Ilzecka J, Stelmasiak Z, Balicka G. Respiratory function in amyotrophic lateral sclerosis. *Neurol Sci* 2003;24:288–289.
5. Singh D, Verma R, Garg RK, Singh MK, Shukla R, Verma SK. Assessment of respiratory functions by spirometry and phrenic nerve studies in patients of amyotrophic lateral sclerosis. *J Neurol Sci* 2011; 306:76–81.
6. Bourke SC, Shaw PJ, Gibson GJ. Respiratory function vs. sleep-disordered breathing as predictors of QOL in ALS. *Neurology* 2001; 57:2040–2044.
7. Lechtzin N, Rothstein J, Clawson L, Diette G, Wiener CM. Amyotrophic lateral sclerosis: evaluation and treatment of respiratory impairment. *Amyotroph Lateral Scler* 2002;3:5–13.
8. Ilieva H, Polymenidou M, Cleveland DW. Non-cell autonomous toxicity in neurodegenerative disorders: ALS and beyond. *J Cell Biol* 2009; 187:761–772.
9. Rothstein JD. Current hypotheses for the underlying biology of amyotrophic lateral sclerosis. *Ann Neurol* 2009;65:S3–S9.
10. Ferraiuolo L, Kirby J, Grierson AJ, Sendtner M, Shaw PJ. Molecular pathways of motor neuron injury in amyotrophic lateral sclerosis. *Nat Rev Neurol* 2011;7:616–630.
11. Yamanaka K, Chun SJ, Boillee S, Fujimori-Tonou N, Yamashita H, Gutmann DH, Takahashi R, Misawa H, Cleveland DW. Astrocytes as determinants of disease progression in inherited amyotrophic lateral sclerosis. *Nat Neurosci* 2008;11:251–253.
12. Lepore AC, Rauck B, Dejea C, Pardo AC, Rao MS, Rothstein JD, Maragakis NJ. Focal transplantation–based astrocyte replacement is neuroprotective in a model of motor neuron disease. *Nat Neurosci* 2008;11:1294–1301.
13. Henriques A, Pitzer C, Schneider A. Neurotrophic growth factors for the treatment of amyotrophic lateral sclerosis: where do we stand? *Front Neurosci* 2010;4:32.
14. Gould TW, Oppenheim RW. Motor neuron trophic factors: therapeutic use in ALS? *Brain Res Brain Res Rev* 2011;67:1–39.
15. Lai EC, Felice KJ, Festoff BW, Gawel MJ, Gelinas DF, Kratz R, Murphy MF, Natter HM, Norris FH, Rudnicki SA; North America ALS/IGF-1 Study Group. Effect of recombinant human insulin-like growth factor-I on progression of ALS: a placebo-controlled study. *Neurology* 1997;49:1621–1630.
16. Borasio GD, Robberecht W, Leigh PN, Emile J, Guiloff RJ, Jerusalem F, Silani V, Vos PE, Wokke JH, Dobbins T; European ALS/IGF-I Study Group. A placebo-controlled trial of insulin-like growth factor-I in amyotrophic lateral sclerosis. *Neurology* 1998;51:583–586.
17. Ochs G, Penn RD, York M, Giess R, Beck M, Tonn J, Haigh J, Malta E, Traub M, Sendtner M, *et al.* A phase I/II trial of recombinant methionyl human brain derived neurotrophic factor administered by intrathecal infusion to patients with amyotrophic lateral sclerosis. *Amyotroph Lateral Scler Other Motor Neuron Disord* 2000;1:201–206.
18. Cedarbaum JM, Stambler N; BDNF Study Group. Disease status and use of ventilatory support by ALS patients. *Amyotroph Lateral Scler Other Motor Neuron Disord* 2001;2:19–22.
19. Beck M, Flachenecker P, Magnus T, Giess R, Reiners K, Toyka KV, Naumann M. Autonomic dysfunction in ALS: a preliminary study on the effects of intrathecal BDNF. *Amyotroph Lateral Scler Other Motor Neuron Disord* 2005;6:100–103.
20. Rosen DR, Siddique T, Patterson D, Figlewicz DA, Sapp P, Hentati A, Donaldson D, Goto J, O'Regan JP, Deng HX. Mutations in Cu/Zn superoxide dismutase gene are associated with familial amyotrophic lateral sclerosis. *Nature* 1993;362:59–62.
21. Baker-Herman TL, Fuller DD, Bavis RW, Zabka AG, Golder FJ, Doperalski NJ, Johnson RA, Watters JJ, Mitchell GS. BDNF is necessary and sufficient for spinal respiratory plasticity following intermittent hypoxia. *Nat Neurosci* 2004;7:48–55.
22. Mitchell GS. Respiratory plasticity following intermittent hypoxia: a guide for novel therapeutic approaches to ventilatory control disorders. In: Gaultier C, editor. Genetic basis for respiratory control disorders. New York: Springer; 2007. pp. 291–306.

23. Klein SM, Behrstock S, McHugh J, Hoffman K, Wallace K, Suzuki M, Aegischer P, Svendsen CN. GDNF delivery using human neural progenitor cells in a rat model of ALS. *Hum Gene Ther* 2005;16:509–521.
24. Suzuki M, McHugh J, Tork C, Shelley B, Klein SM, Aebischer P, Svendsen CN. GDNF secreting human neural progenitor cells protect dying motor neurons, but not their projection to muscle, in a rat model of familial ALS. *PLoS One* 2007;2:e689.
25. Satriotomo I, Nashold LJ, Svendsen CN, Mitchell GS. Enhancement of BDNF and serotonin terminal density in phrenic and hypoglossal motor nuclei in a rat model of amyotrophic lateral sclerosis (ALS) [abstract]. *FASEB J* 2006;20:A1212.
26. Gowing G, Nichols NL, Suzuki M, McHugh J, Hayes A, Mulcrone P, Mitchell GS, Svendsen CN. Targeting of human neural progenitor cells expressing GDNF to the cervical spinal cord of a rat model of ALS [abstract]. *Soc Neurosci Abstr* 2010;753.11.
27. Nichols NL, Gowing G, Suzuki M, Svendsen CN, Mitchell GS. GDNF-secreting stem cell implants strengthen phrenic motor output in $SOD1^{G93A}$ rats [abstract]. *Soc Neurosci Abstr* 2010;753.10.
28. Lovett-Barr MR, Satriotomo I, Muir G, Wilkerson JER, Hoffman MS, Vinit S, Mitchell GS. Repetitive intermittent hypoxia induces respiratory and somatic motor recovery following chronic cervical spinal injury. *J Neurosci* 2012;32:3591–3600.
29. Hoffman MS, Mitchell GS. Spinal 5-HT receptor activation induces long-lasting phrenic motor facilitation. *J Physiol* 2011;589:1397–1407.
30. Mantilla CB, Zhan WZ, Sieck GC. Retrograde labeling of phrenic motoneurons by intrapleural injection. *J Neurosci Methods* 2009;182:244–249.
31. Boulenguez P, Gestreau C, Vinit S, Stamegna JC, Kastner A, Gauthier P. Specific and artifactual labeling in the rat spinal cord and medulla after injection of monosynaptic retrograde tracers into the diaphragm. *Neurosci Lett* 2007;417:206–211.
32. Svendsen CN, Caldwell MA, Shen J, ter Borg MG, Rosser AE, Tyers P, Karmiol S, Dunnet SB. Long-term survival of human central nervous system progenitor cells transplanted into a rat model of Parkinson's disease. *Exp Neurol* 1997;148:135–146.
33. Svendsen CN, ter Borg MG, Armstrong RJ, Rosser AE, Chandran S, Ostenfeld T, Caldwell MA. A new method for the rapid and long term growth of human neural precursor cells. *J Neurosci Methods* 1998;85:141–152.
34. Déglon N, Tseng JL, Bensadoun JC, Zurn AD, Arsenijevic Y, Pereira de Almeida L, Zufferey R, Trono D, Aebischer P. Self-inactivating lentiviral vectors with enhanced transgene expression as potential gene transfer system in Parkinson's disease. *Hum Gene Ther* 2000;11:179–190.
35. Tankersley CG, Haenggeli C, Rothstein JD. Respiratory impairment in a mouse model of amyotrophic lateral sclerosis. *J Appl Physiol* 2007;102:926–932.
36. Llado J, Haenggeli C, Pardo A, Wong V, Benson L, Coccia C, Rothstein JD, Shefner JM, Maragakis NJ. Degeneration of respiratory motor neurons in the SOD1 G93A transgenic rat model of ALS. *Neurobiol Dis* 2005;21:110–118.
37. Golder FJ, Mitchell GS. Spinal synaptic enhancement with acute intermittent hypoxia improves respiratory function after chronic cervical spinal cord injury. *J Neurosci* 2005;25:2925–2932.
38. Dale-Nagle EA, Satriotomo I, Mitchell GS. Spinal vascular endothelial growth factor induces phrenic motor facilitation via extracellular signal–regulated kinase and Akt signaling. *J Neurosci* 2011;31:7682–7690.
39. Dale EA, Satriotomo I, Mitchell G. Cervical spinal erythropoietin induces phrenic motor facilitation via extracellular signal–regulated protein kinase and Akt signaling. *J Neurosci* 2012;32:5973–5983.
40. Satriotomo I, Dale EA, Dahlberg JM, Mitchell GS. Repetitive acute intermittent hypoxia increases expression of proteins associated with plasticity in the phrenic motor nucleus. *Exp Neurol* 2012;237:103–115.
41. Yanpallewar SU, Barrick CA, Buckley H, Becker J, Tessarollo L. Deletion of the BDNF truncated receptor TrkB.T1 delays disease onset in a mouse model of amyotrophic lateral sclerosis. *PLoS ONE* 2012;7:e39946.
42. Oppenheim RW, Houenou LJ, Parsadanian AS, Prevette D, Snider WD, Shen L. Glial cell line–derived neurotrophic factor and developing mammalian motoneurons: regulation of programmed cell death among motoneuron subtypes. *J Neurosci* 2000;20:5001–5011.
43. Kanning KC, Kaplan A, Henderson CE. Motor neuron diversity in development and disease. *Annu Rev Neurosci* 2010;33:409–440.
44. Jessell TM. Neuronal specification in the spinal cord: inductive signals and transcriptional codes. *Nat Rev Genet* 2000;1:20–29.
45. Liu JP, Laufer E, Jessell TM. Assigning the positional identity of spinal motor neurons: rostrocaudal patterning of Hox-c protein expression by FGFs, Gdf11 and retinoids. *Neuron* 2001;32:997–1012.
46. Alaynick WA, Jessell TM, Pfaff SL. Snapshot: spinal cord development. *Cell* 2011;146:178.
47. Ostenfeld T, Caldwell MA, Prowse KR, Linskens MH, Jauniaux E, Svendsen CN. Human neural precursor cells express low levels of telomerase *in vitro* and show diminishing cell proliferation with extensive axonal outgrowth following transplantation. *Exp Neurol* 2000;164:215–226.
48. Lepore AC, O'Donnell J, Kim AS, Williams T, Tuteja A, Rao MS, Kelley LL, Campanelli JT, Maragakis NJ. Human glial-restricted progenitor transplantation into cervical spinal cord of the SOD1 mouse model of ALS. *PLoS One* 2011;6:e25968.
49. Trumbower RD, Jayaraman A, Mitchell GS, Rymer WZ. Exposure to acute intermittent hypoxia augments somatic motor function in humans with incomplete spinal cord injury. *Neurorehabil Neural Repair* 2012;26:163–172.
50. Boulis NM, Federici T, Glass JD, Lunn JS, Sakowski SA, Feldman EL. Translational stem cell therapy for amyotrophic lateral sclerosis. *Nat Rev Neurol* 2011;8:172–176.
51. Lunn JS, Sakowski SA, Federici T, Glass JD, Boulis NM, Feldman EL. Stem cell technology for the study and treatment of motor neuron diseases. *Regen Med* 2011;6:201–213.